EPJ Web of Conferences **316**, 01012 (2025) https://doi.org/10.1051/epjconf/202531601012
SQM 2024

Experimental overview on light (anti)(hyper)nuclei production at the LHC

Chiara Pinto[1,*]

[1]European Organisation for Nuclear Research (CERN), Geneva, Switzerland

Abstract. For many years, significant efforts at the LHC have been put towards the measurements of the production of (anti)(hyper)nuclei in high-energy hadronic collisions. The ALICE experiment has contributed with measurements in pp, p–Pb, Xe–Xe, and Pb–Pb collisions, at various center-of-mass energies. Recently, also the LHCb experiment has measured the production of nuclei in both collider and fixed-target modes. The highlights of recent experimental measurements are discussed in the context of the production models used to describe the hadronization mechanism.

1 Introduction

At the Large Hadron Collider, the baryochemical potential is close to zero [1] and therefore it is possible to measure the production of both nuclei and antinuclei, in several collision systems, from pp to Pb–Pb, in a range of center-of-mass energies between $\sim$ 1 and $\sim$ 13 TeV. The measurements of the production of (anti)(hyper)nuclei at accelerators allow the study of the nucleosynthesis mechanism, which is nowadays under intense debate in the scientific community. The production mechanism is usually described by three classes of phenomenological models, i.e., the statistical hadronization model (SHM), the coalescence approach, and hybrid models that include relativistic hydrodynamics with a subsequent coalescence afterburner, to describe the survival of bound states in the hadron gas phase with intense rescattering. Many observables have been pointed out to have a strong discrimination power among the model predictions, and therefore the experimental challenge today is to get the most possibly precise measurement to compare to the expectations of the models. Besides the interest in the hadronization mechanism per se, the study of the production of (anti)(hyper)nuclei at the LHC has important applications to the indirect dark matter searches and to the study of the particle interactions needed for the equation of state to describe neutron star observations.

2 Testing production models

According to SHM, light (anti)(hyper)nuclei are produced by a source in local thermal and hadrochemical equilibrium at the chemical freeze-out, with a temperature common to all light flavor species [2], of about 155 MeV. Such chemical freeze-out temperature corresponds to the phase-transition temperature, that is the same in Pb–Pb [3] and Xe–Xe [4] collisions, and corresponds to the pseudo-critical temperature for the transition from QGP to hadron

*e-mail: chiara.pinto@cern.ch

gas predicted by lattice QCD calculations [5]. In heavy-ion collisions, the grand-canonical ensemble of the statistical model [2, 6, 7], where all the charges are only conserved on average but fluctuate from one microscopic state to another, holds true to describe the particle yield in the case of sufficiently large reaction volumes. In small collision systems (e.g., pp and p–Pb collisions), the exact conservation of charges from one microscopic state to another plays an important role in determining the final state particle yield. Therefore, the canonical ensemble of the SHM is used, resulting in the so-called canonical suppression of the yields of particles carrying conserved charges, relative to their grand-canonical values.

In the coalescence model, light (anti)(hyper)nuclei are formed by the coalescence of nucleons that are close in phase space and with matching spin-isospin configurations, at kinetic freeze-out (occurring when the elastic interactions stop and the momentum of the particles is fixed). In the state-of-the-art implementation of the coalescence model, the formation probability is calculated by folding the phase-space distributions of the constituent nucleons with the Wigner density distribution of the bound state [8].

Recent developments of the coalescence model based on the Wigner function formalism have shown that the coalescence of deuterons is extremely sensitive to the wavefunction of the nucleus and to the size of the baryon-emitting source [7–9]. For instance, in order to reproduce the measured transverse momentum distribution of deuterons measured in the high-multiplicity sample of pp collisions at a center-of-mass energy of $\sqrt{s}$ = 13 TeV by ALICE with a coalescence model based on the Wigner function formalism [8], the realistic wavefunction of deuterons, i.e., Argonne v18 [10], is needed in addition to the measured baryon-emitting source size [11], as shown in Fig. 1.

On the contrary, the SHM predictions depend only on the mass and on the spin degeneracy factor of the nucleus. This aspect is particularly relevant in two cases: (i) in small collision systems, since the size of the nucleus (r_{deuteron} = 1.96 fm and $r_{^3\text{He}}$ = 1.76 fm [12]) and that of the baryon-emitting source ($r \sim 1$ fm in pp collisions [13] and $r \sim 1.5$ fm in p–Pb colli-

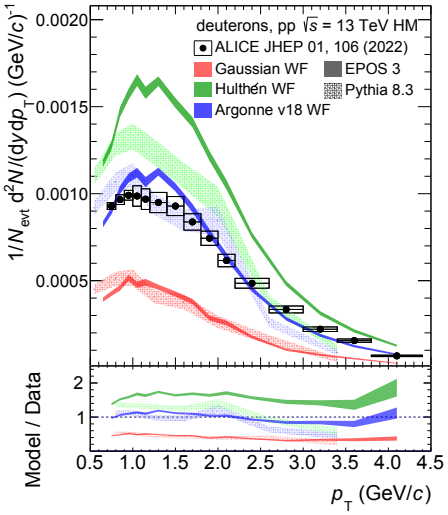

Figure 1. Transverse momentum distribution of deuterons measured in the high multiplicity class of pp collisions at $\sqrt{s}$ = 13 TeV by ALICE, compared to the expectations of a coalescence model based on the Wigner function formalism that uses several hypotheses for the wavefunction, implemented as an afterburner on top of events generated with EPOS 3 or PYTHIA 8.3.

sions [14]) are comparable; (ii) in the ratios of the yields of nuclei and hypernuclei with mass number $A \geq 3$.

In the left panel of Figure 2 the ratios of the integrated yields of deuterons and protons are shown as a function of the charged-particle multiplicity and compared to the expectations of the production models. The predictions of two implementations of the canonical statistical model (CSM) with different hypotheses for the freeze-out temperature and those of the coalescence model describe qualitatively the smoothly increasing trend of the deuteron-to-proton yield ratios with multiplicity and the overall yields. Notably, all the predictions give similar results for the $A = 2$ yield ratios, making it difficult to discriminate among the hadronization mechanisms. A better discrimination power is present for the ratios of ^{3}He-to-proton yields, as shown in the right panel of Fig. 2: especially at the multiplicities corresponding to heavy-ion collisions, models differ by $\sim 40\%$. However, the current experimental precision is not enough to distinguish among the predictions of the different models.

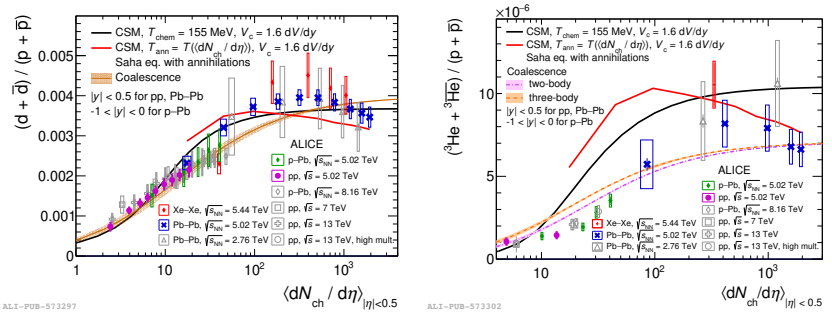

Figure 2. The ratios of the integrated yields of deuterons and protons (left panel) and ^{3}He and protons (right panel) are shown as a function of the charged-particle multiplicity and compared to the expectations of several production models.

In this scenario, hypernuclei (nuclei with at least one hyperon constituent) play an important role as they are very loosely bound states with a large spatial extension of their wavefunction. For instance, hypertriton is a hypernucleus composed of a proton, a neutron, and a Λ hyperon, with a separation energy of the Λ of about 102 keV [15] and a radius of about 10 fm [16]. The ratio of the yields of the $^3_\Lambda$H and of the ^{3}He as a function of multiplicity has a great discrimination power between the SHM and coalescence (see left panel of Fig. 3), because the two species have comparable masses ($m_{^3_\Lambda\mathrm{H}}$=2.991 and $m_{^3\mathrm{He}}$=2.809 GeV/c^2) but very different sizes ($r_{^3_\Lambda\mathrm{H}}$ ~10 fm and $r_{^3\mathrm{He}}$=1.76 fm). Hence, the SHM, which depends only on the masses of the nuclei, predicts a flat ratio as a function of multiplicity, while the coalescence model, which takes into account the interplay between the source size and the spatial extension of the nucleus wavefunction, results in an increasing trend of the predicted ratio as a function of multiplicity, that reflects the increasing size of the baryon-emitting source. Finally, another powerful tool to discriminate among the predictions of the production models is the multiplicity-dependent ratio of the yields of $^3_\Lambda$H and those of the Λ baryon. The models give very different predictions for such a ratio, especially in the low multiplicity range, corresponding to small systems. Only few measurements of this ratio are currently available from the ALICE Collaboration, as shown in the right panel of Fig. 3, but with a precision good enough to discriminate among the models. The data agrees with the predictions of the coalescence model within 1σ at $\langle \mathrm{d}N_{\mathrm{ch}}/\mathrm{d}\eta \rangle < 10$, and exclude the SHM predictions by $\sim 6\sigma$.

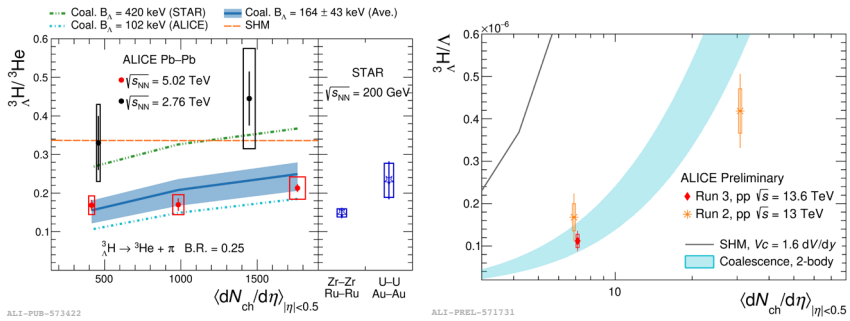

Figure 3. Ratio of the integrated yields of ${}^{3}_{\Lambda}\mathrm{H}$ and ${}^{3}\mathrm{He}$ (left panel) and of ${}^{3}_{\Lambda}\mathrm{H}$ and Λ (right panel) as a function of the charged-particle multiplicity, compared to the expectations of different production models.

3 Impact on astrophysics

One interesting application of the measurement of the production of antinuclei in accelerator experiments concerns the search for indirect dark matter (DM). Antinuclei in the Galaxy might be produced either by reactions of primary cosmic rays (CRs) with the interstellar medium (ISM), both constituted for the 90% by protons and for the 9% by alpha nuclei, or by annihilation of dark matter candidates, or by even more exotic sources such as anticlouds or antistars [17]. Although antinuclei heavier than antiprotons still elude detection in space, many theoretical efforts are ongoing in order to model the flux of antinuclei from cosmic rays, with the ultimate goal of correctly interpret any future measurement of antinuclear CR fluxes. In this sense, information on the production of antinuclei from accelerator experiments, particularly in small collision systems, is essential for the theoretical description of the background constituted by antinuclei from cosmic-ray collisions with ISM. Notably, the production of antinuclei at the LHC is typically measured at midrapidity ($|y| < 0.5$), and then, combined with several coalescence models, employed to predict the flux of antinuclei from CR interactions at forward rapidity. However, the possible impact of a rapidity dependence of the production yield and of the coalescence probability[1] of antinuclei was suggested in Ref. [18] and recently investigated by the ALICE Collaboration in pp collisions at $\sqrt{s} = 13$ TeV [19]. In such work, the rapidity dependence of the production yield of $\overline{\mathrm{p}}$ and $\overline{\mathrm{d}}$ and of the coalescence parameter B_2 (obtained from Eq. 1 with $A = 2$) has been investigated. The measurements have been carried out rapidity-differentially up to $|y| < 0.7$, and then, with the use of the a state-of-the-art coalescence model based on the Wigner formalism [8], the integrated yields and B_2 have been extrapolated to forward rapidity and high p_{T}, as shown in Fig. 4. These model predictions have been used as input for the calculations of the flux of antinuclei from cosmic rays in Ref. [20]. In such work, the author investigates the role of the rapidity extrapolation in the predictions of the CR flux of antinuclei assessing that about 90% of the flux is due to antideuterons with rapidity between 0.5 and 1.5. This kinematical region is the one where the CR flux is expected to be dominated by the DM signal, according

[1]The coalescence parameter is defined as the ratio between the invariant yield of the nucleus with mass number A and that of the protons, raised to the power of A, assuming protons and neutrons to have the same transverse momentum distributions as they are isospin partners, and $p_{\mathrm{T}}^{\mathrm{p}} = p_{\mathrm{T}}^{A}/A$:

$$B_A = \left(\frac{1}{2\pi p_{\mathrm{T}}^{A}}\left(\frac{\mathrm{d}^2N}{\mathrm{d}y\mathrm{d}p_{\mathrm{T}}}\right)_A\right)\Big/\left(\frac{1}{2\pi p_{\mathrm{T}}^{\mathrm{p}}}\left(\frac{\mathrm{d}^2N}{\mathrm{d}y\mathrm{d}p_{\mathrm{T}}}\right)_{\mathrm{p}}\right)^{A}. \quad (1)$$

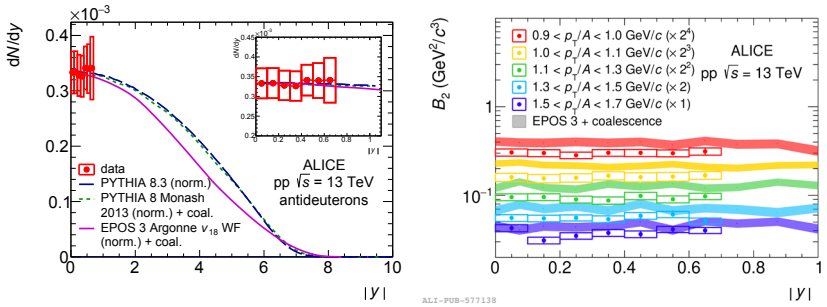

Figure 4. Deuteron yields (left panel) and coalescence parameter B_2 as a function of rapidity for fixed intervals of the p_T/A (right panel), measured in pp collisions at $\sqrt{s}$ = 13 TeV by ALICE [19]. The data are compared to the predictions of a coalescence afterburner based on the Wigner function formalism, on top of events generated with EPOS 3 or PYTHIA.

to many cosmological models [21]. The relevant rapidity region ($0.5 < |y| < 1.5$) is in reach of present or future LHC experiments, such as LHCb [22] in its fixed-target configuration, CMS [23] in its Run 4 program, and the future ALICE 3 facility [24].

Finally, one open point is still the extrapolation to the low-energy scale needed for astrophysical models: while the LHC experiments cover the TeV scale, the production of antinuclei in the Galaxy occurs at center-of-mass energies of the order of 1–10 GeV (for instance, antideuterons are produced in collisions of $\sqrt{s}$ = 17 GeV [21]). The current assumption is that the production models employed at the LHC energy scale can also be used at lower energies. The LHCb Collaboration recently measured ^{3}He nuclei [25] and successfully identified (anti)hypertritons [26]. Future (anti)deuteron and (anti)^{3}He measurements as a function of rapidity provided by LHCb would be highly useful for the cosmic-ray flux modeling, as the LHCb fixed-target mode would allow the scan of the low energy collision range (of the order of 1–10 GeV), relevant for astrophysics.

References

[1] S. Acharya et al. (ALICE), Measurements of chemical potentials in Pb-Pb collisions at $\sqrt{s_{\rm NN}}$ = 5.02 TeV (2023), 2311.13332.

[2] A. Andronic, P. Braun-Munzinger, K. Redlich, J. Stachel, Decoding the phase structure of QCD via particle production at high energy, Nature **561**, 321 (2018), 1710.09425. 10.1038/s41586-018-0491-6

[3] A. Andronic, P. Braun-Munzinger, B. Friman, P.M. Lo, K. Redlich, J. Stachel, The thermal proton yield anomaly in Pb–Pb collisions at the LHC and its resolution, Phys. Lett. B **792**, 304 (2019), 1808.03102. 10.1016/j.physletb.2019.03.052

[4] S. Acharya et al. (ALICE), Measurement of the production and elliptic flow of (anti)nuclei in Xe-Xe collisions at $\sqrt{s_{\rm NN}}$ = 5.44 TeV (2024), 2405.19826.

[5] A. Bazavov et al. (HotQCD), Chiral crossover in QCD at zero and non-zero chemical potentials, Phys. Lett. B **795**, 15 (2019), 1812.08235. 10.1016/j.physletb.2019.05.013

[6] F. Bellini, A.P. Kalweit, Testing production scenarios for (anti-)(hyper-)nuclei and exotica at energies available at the CERN Large Hadron Collider, Phys. Rev. C **99**, 054905 (2019), 1807.05894. 10.1103/PhysRevC.99.054905

[7] R. Scheibl, U.W. Heinz, Coalescence and flow in ultrarelativistic heavy ion collisions, Phys. Rev. **C59**, 1585 (1999), nucl-th/9809092. 10.1103/PhysRevC.59.1585

[8] M. Mahlein, L. Barioglio, F. Bellini, L. Fabbietti, C. Pinto, B. Singh, S. Tripathy, A realistic coalescence model for deuteron production, Eur. Phys. J. C **83**, 804 (2023), 2302.12696. 10.1140/epjc/s10052-023-11972-3

[9] H. Sato, K. Yazaki, On the coalescence model for high energy nuclear reactions, Phys. Lett. B **98**, 153 (1981). https://doi.org/10.1016/0370-2693(81)90976-X

[10] R.B. Wiringa, V.G.J. Stoks, R. Schiavilla, Accurate nucleon-nucleon potential with charge-independence breaking, Phys. Rev. C **51**, 38 (1995). 10.1103/PhysRevC.51.38

[11] S. Acharya et al. (ALICE), Search for a common baryon source in high-multiplicity pp collisions at the LHC, Phys. Lett. B **811**, 135849 (2020), 2004.08018. 10.1016/j.physletb.2020.135849

[12] G. Ropke, Light nuclei quasiparticle energy shift in hot and dense nuclear matter, Phys. Rev. C **79**, 014002 (2009), 0810.4645. 10.1103/PhysRevC.79.014002

[13] S. Acharya et al. (ALICE), p-p, p-Λ and Λ-Λ correlations studied via femtoscopy in pp reactions at $\sqrt{s} = 7$ TeV, Phys. Rev. C **99**, 024001 (2019), 1805.12455. 10.1103/PhysRevC.99.024001

[14] S. Acharya et al. (ALICE), First Observation of an Attractive Interaction between a Proton and a Cascade Baryon, Phys. Rev. Lett. **123**, 112002 (2019), 1904.12198. 10.1103/PhysRevLett.123.112002

[15] S. Acharya et al. (ALICE), Measurement of the Lifetime and Λ Separation Energy of HΛ3, Phys. Rev. Lett. **131**, 102302 (2023), 2209.07360. 10.1103/PhysRevLett.131.102302

[16] F. Hildenbrand, H.W. Hammer, Three-Body Hypernuclei in Pionless Effective Field Theory, Phys. Rev. C **100**, 034002 (2019), [Erratum: Phys.Rev.C 102, 039901 (2020)], 1904.05818. 10.1103/PhysRevC.100.034002

[17] V. Poulin, P. Salati, I. Cholis, M. Kamionkowski, J. Silk, Where do the AMS-02 antihelium events come from?, Phys. Rev. D **99**, 023016 (2019), 1808.08961. 10.1103/PhysRevD.99.023016

[18] Z. Citron et al., Report from Working Group 5: Future physics opportunities for high-density QCD at the LHC with heavy-ion and proton beams, CERN Yellow Rep. Monogr. **7**, 1159 (2019), 1812.06772. 10.23731/CYRM-2019-007.1159

[19] S. Acharya et al. (ALICE), Rapidity dependence of antideuteron coalescence in pp collisions at $\sqrt{s} = 13$ TeV with ALICE (2024), 2407.10527.

[20] K. Blum, Rapidity dependence of nuclear coalescence: Impact on cosmic ray antinuclei, Phys. Rev. C **109**, L031904 (2024), 2306.13165. 10.1103/PhysRevC.109.L031904

[21] L. Šerkšnytė et al., Reevaluation of the cosmic antideuteron flux from cosmic-ray interactions and from exotic sources, Phys. Rev. D **105**, 083021 (2022), 2201.00925. 10.1103/PhysRevD.105.083021

[22] A.A. Alves, Jr. et al. (LHCb), The LHCb Detector at the LHC, JINST **3**, S08005 (2008). 10.1088/1748-0221/3/08/S08005

[23] New opportunities of heavy ion physics with CMS-MTD at the HL-LHC (2021), https://cds.cern.ch/record/2800541

[24] Letter of intent for ALICE 3: A next-generation heavy-ion experiment at the LHC (2022), 2211.02491

[25] R. Aaij et al. (LHCb), Helium identification with LHCb, JINST **19**, P02010 (2024), 2310.05864. 10.1088/1748-0221/19/02/P02010

[26] H. Jage, Observation of antihelium and antihypertriton in pp collisions with LHCb, PoS **EPS-HEP2023**, 254 (2024). 10.22323/1.449.0254